Interfacial Reaction and Microstructural Evolution between Au-Ge Solder and Electroless Ni-W-P Metallization in High Temperature Electronics Interconnects

Li Liu[1,4*], Jing Wang[1], Changqing Liu[1*]
[1] Wolfson School of Mechanical, Electrical and Manufacturing Engineering, Loughborough University
Loughborough, LE11 3TU, UK.
[4] School of Materials Science and Engineering, Wuhan University of Technology
122 Luoshi Road, Wuhan, 430070, China
E-mail*: C.Liu@lboro.ac.uk (or) L.Liu@whut.edu.cn,
Phone: +44-(0)1509227639

Jinzi Cui[2], Zhaoxia Zhou[3], R. Wayne Johnson[2,5]
[2] Department of Electrical and Computer Engineering, Auburn University
Broun Hall, 341 War Eagle Way, Auburn, AL 36849, USA
[3] Loughborough Materials Characterisation Centre, Loughborough, LE11 3TU, UK
[5] Electrical and Computer Engineering Department, Tennessee Technological University
Box 5004, 115 W. 10th St. Brown Hall, Cookeville, TN 38505, USA
Email: wjohnson@tntech.edu, Phone: +1 931-372-3397

***Abstract*—The elevated working temperature of high temperature electronics can inevitably cause potential excessive growth of interfacial intermetallic compounds (IMCs), which can significantly deteriorate the mechanical integrity of electronic devices. Therefore, a robust diffusion barrier that can operate reliably under elevated temperature is highly demanded to retard the interfacial reaction between solder and substrate. In this work, a ternary Ni-W-P alloy was deposited through electroless plating and applied as an Under Bump Metalisation (UBM) to Au-Ge solder joints. The interfacial reaction in Au-Ge/Ni-W-P solder joints after reflow and prolonged ageing durations was investigated. We found NiGe and Ni_5Ge_3 layers formed after reflow, however only NiGe was observed after 1000h aging at 300ºC. The thickness of NiGe increases linearly with the square root of ageing time up to 1500h, indicating that the growth mechanism of NiGe is diffusion-control process when Ge atoms are sufficient. After ageing for 2000h, although Ge atoms from Au-Ge solder was fully consumed, the Ni-W-P coating remained stable and exhibited excellent diffusion barrier property. During various ageing durations, the top-view morphology of NiGe IMC grains changed from pyramid-like and polygon-like shape at as-built stage to granulate-like (up to 1500h), and finally a polygon-like shape (after 2000h).**

Keywords-Electroless Ni-W-P coating; Au-Ge solder; Interfacial reaction; morphological evolution

I. INTRODUCTION

The demand for high temperature power electronics that are capable of operating under high power density and high temperature continues to grow, particularly in the applications of aerospace, automotive and drilling devices. During reflow process, intermetallic compounds (IMCs) can be produced through the reactions between solder and the metallisation to form a solder joint. Although the formation of initial IMCs can establish a good metallurgical bond between high temperature solder and substrate, excessive growth of IMCs during ageing process would significantly deteriorate the interfacial integrity, due to the differences of physical properties (e.g. elastic modulus and coefficient of thermal expansion) of solders involved [1, 2]. This is particularly true in high temperature electronics, because the devices normally operate at elevated temperature that can significantly accelerate the growth of IMCs. Hence, a reliable under bump metallisation (UBM) to retard the interfacial reaction rate is of vital importance.

Currently, the most widely used UBM in electronic applications is electroless Ni-P coating as a diffusion barrier to retard the interfacial reaction rate. However, when operated at elevated temperature (up to 300ºC) in high temperature electronics, the Ni-P coating can produce a columnar-structure Ni_3P layer with enormous nano-voids embedded, resulting in great deterioration in its diffusion barrier property [3-5]. For instance, in typical high temperature Au-Ge solder joints, electroless Ni-P coatings (thickness: 5 µm) were reported to be completely consumed by the growth of Ni-Ge intermetallic compounds (IMCs) at 300ºC for 1000 hours [6].

Therefore, a novel metallisation that can keep stable under relatively high temperature (at least above 300°C) is highly desirable in applications of high temperature electronics. It is reported that an incorporation of a refractory metal element (W) in binary Ni-P alloy through electroless deposition can significantly enhance the crystallisation characteristics and thermal stability of binary Ni-P alloy [7-9]. To date, few researches have been carried out on the reactions between Ni-W-P interlayer with Sn-Bi or Sn-3.5Ag solders, drawing a conclusion that the interfacial reactions in Ni-W-P solder joints are obviously slower than those with a Ni-P interlayer after long-term ageing durations [8, 10, 11]. Notably, these solders are generally applied in a relatively low-temperature regime (peak reflow temperature < 220°C). So far, the interfacial reactions between electroless Ni-W-P coatings and high-temperature solders after reflow and prolonged ageing has seldom been reported from the author's knowledge.

In this work, a ternary Ni-W-P alloy was prepared through electroless plating, which is a simple preparation process and suitable for industrial applications. Its morphology and composition was studied with scanning electron microscopy (SEM). The interfacial reaction and microstructural evolution between Ni-W-P coating and typical Au-Ge high temperature solder after prolonged ageing process (up to 2000h at 300ºC) were also examined with the aid of SEM, Focused Ion Beam (FIB) and Transmission Electron Microscopy (TEM). The growth mechanism of the interfacial IMC layer was finally proposed.

II. Experimental

In this work, 96% aluminum oxide direct bond copper (DBC) boards (Stellar Industry, Millbury, USA) were used as the substrates for electroless Ni-W-P plating. The thickness of Al_2O_3 layer and Cu foil on DBC boards was 0.635 mm and 0.2032 mm, respectively. The area size of this Cu foil was around 60 mm × 63 mm. The eletroless Ni-W-P plating was carried out in an alkaline bath with a pH value of 8.2 (adjusted with dilute H_2SO_4 and NaOH solution) at 83 ± 2°C for 10 minutes. Table 1 lists the formulations of this electroless Ni-W-P plating solution. The sources of Ni and W elements were nickel sulphate ($NiSO_4$) and sodium tungstate (Na_2WO_4), respectively. Sodium hypophosphite (NaH_2PO_2) worked as a reducing agent, while sodium citrate ($Na_3C_6H_5O_7$) acted as a complexing agent. In addition, sodium lauryl sulphate (SLS, $CH_3(CH_2)_{11}OSO_3Na$) was added into the bath in a small amount of 0.3 mg/L to eliminate the pinholes and pores in Ni-W-P coatings for a better surface quality [11].

TABLE 1 COMPOSITION OF THE ELECTROLESS NI-W-P PLATING BATH.

Chemical reagents	Concentration (g/L)
$NiSO_4 \cdot 6H_2O$	7
$Na_2WO_4 \cdot 2H_20$	35
$NaH_2PO_2 \cdot H_20$	10
$Na_3C_6H_5O_7 \cdot 2H_2O$	40
$CH_3(CH_2)_{11}OSO_3Na$	3×10^{-4}

After electroless Ni-W-P plating, sandwich-structure SiC/Au-Ge/Ni-W-P solder joints were performed in a SST vacuum furnace with three minutes ramping from room temperature (25°C) to 385°C, followed with three minutes dwelling at 385°C for achieving a good wetting performance. Afterwards, the solder joints were cold-mounted, ground and final polished with 1 μm colloidal silica particles for interfacial observations. Moreover, to obtain top-view morphology of IMCs, a deep etched method with a combined etchant of 400 g KI, 200 g I_2 and 1000 ml DI water was applied on Au-Ge solder joints for 15 minutes prior to SEM observations. The interfacial microstructure and IMC morphology in these solder interfaces were observed with a FEG-SEM (Carl Zeiss, Stereoscan 360, Cambridge), using back-scattered electron (BSE) mode. The composition and diffusion profile at the solder interfaces were characterised by an energy dispersive X-ray (EDX) spectrometer. However, due to the thin thickness (< 1 μm) of the interfacial IMCs layer in as-built specimen, FEG-SEM technique is not sufficient to clarify the reaction mechanisms between solders and electroless Ni-W-P coatings for the unclear resolutions and inaccurate EDX analysis in high magnifications (above 20000×). Therefore, a dual-beam focus ion beam (FIB, FEI Nova 600 Nanolab Dual Beam) was used to fabricate the samples for transmission electron microscopy (TEM, JEOL 2000FX) analysis at a nano-scale. Finally, an in-depth material analysis can be conducted at the Ni-W-P/Au-Ge interfaces through TEM technique.

III. Results and Discussion

A. As-deposited Ni-W-P metallisation

The EDX results of as-deposited Ni-W-P coatings are listed in Table 2. The P content ranged within 6-7 wt.% and the W content was within 15-16 wt.%. Fig. 1 shows the surface morphology and cross-section of the electroless Ni-W-P coatings. In Fig. 1a), the surface contains smooth nodules with an uneven size range of 1 μm - 3 μm. No pores can be observed on its surface. In Fig. 1 b), the thickness of this coating is approximately 3.8 μm. It was closely adhered to the Cu substrate, while no pores or cracking were found at the Ni-W-P/Cu interface. Overall, this Ni-W-P coating was crack-free, compact and adherent, exhibiting a good morphology quality as a diffusion barrier.

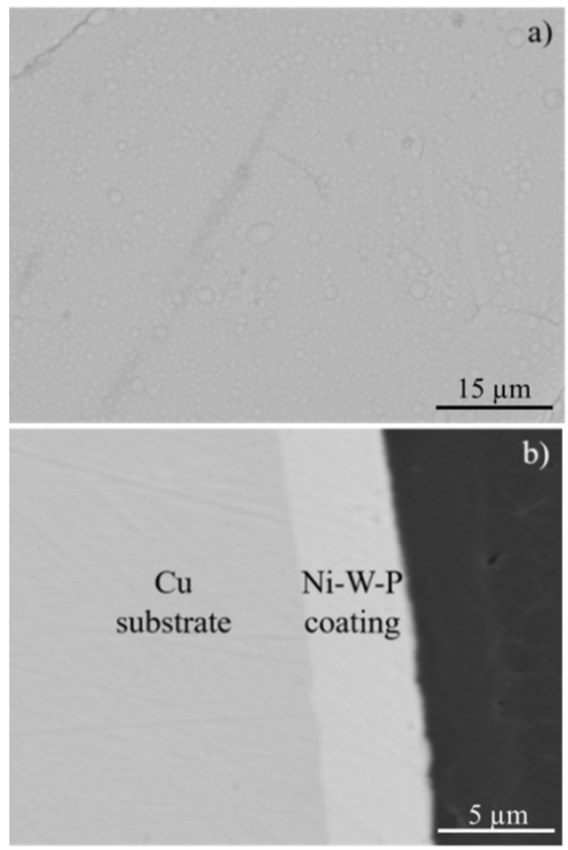

Fig. 1. Micrographs of the as-deposited Ni-W-P coating: a) surface morphology; b) cross-section morphology.

TABLE 2. COMPOSITION OF AS-DEPOSITED NI-W-P COATINGS THROUGH EDX ANALYSIS (WT.%)

Spectrum	Ni	W	P
1	77.8	15.4	6.8
2	76.7	15.9	7.4
3	77.4	15.6	7.0

B. Interfacial reaction and IMC morphology in as-assembled Au-Ge solder joints

Fig. 2 shows the cross-section micrograph of the as-assembled Au-Ge solder joints. In Fig. 2 a), the SiC die horizontally bonds on Cu foil through a thin layer of die attachment. On enlarged Region b, the thickness of this die attachment is approximately 14 µm in Fig. 2 b), consisting of Au-Ge solder, Ni-Ge IMCs and some dispersive Ge-rich phases pointed out by white arrows. Notably, several voids were observed along boundaries of some Ni-Ge IMC grains and the Ni-W-P coatings, which is likely to induce the separation of Ni-Ge IMCs under shear loads.

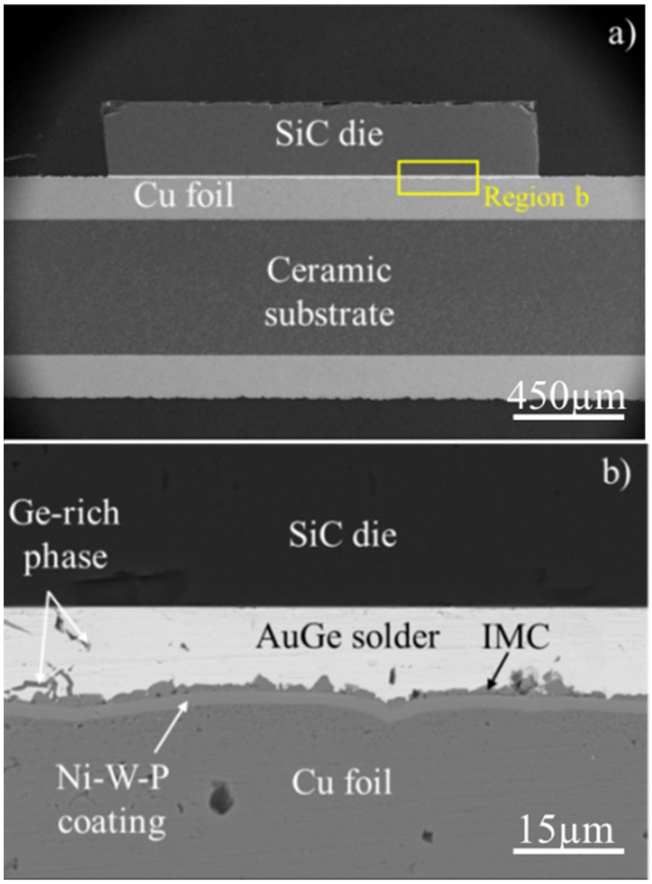

Fig. 2. Cross-section SEM images of as-assembled Au-Ge solder joints: a) Overview of entire joints, b) enlarge view of Region b (back-scattered electron mode).

Elemental mapping analysis was conducted on this solder interface and the results are illustrated in Fig. 3. It is clearly observed that nickel (Ni) atoms diffuse out from the Ni-W-P coating to form Ni-Ge IMCs with germanium (Ge) atoms from the Au-Ge solder. The thickness of entire Ni-Ge IMCs layer was rather thin at approximately 1 µm. According to elemental mapping results, no Cu elements were found within the Au-Ge solder, while Au atoms were also not observed in the Cu substrate. This indicates that Ni-W-P coating is an excellent diffusion barrier to prevent the mutual diffusions and reactions between Cu substrates and Au-Ge solders.

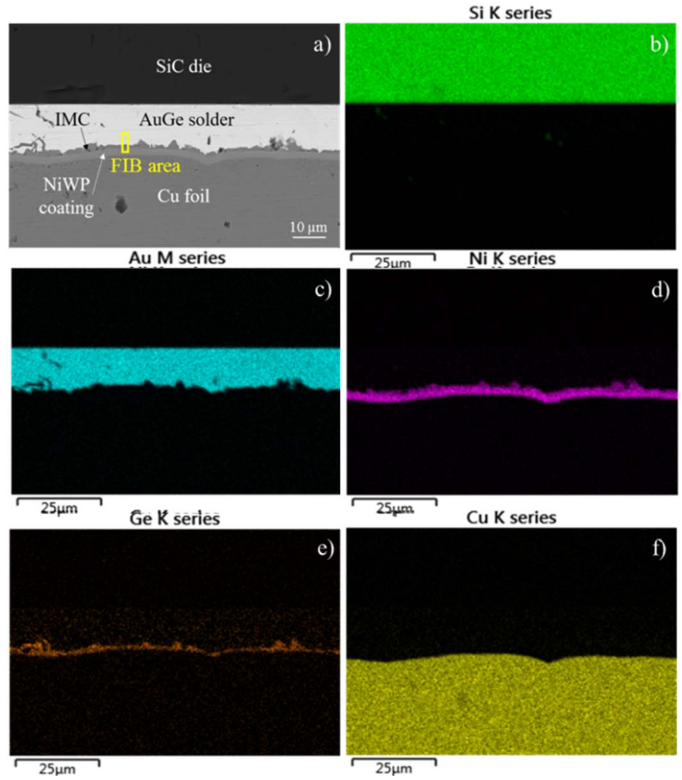

Fig. 3. EDX element mapping analysis of the Au-Ge solder joints: a) back-scattered SEM image, b) mapping for Si, c) mapping for Au, d) mapping for Ni, e) mapping for Ge, f) mapping for Cu.

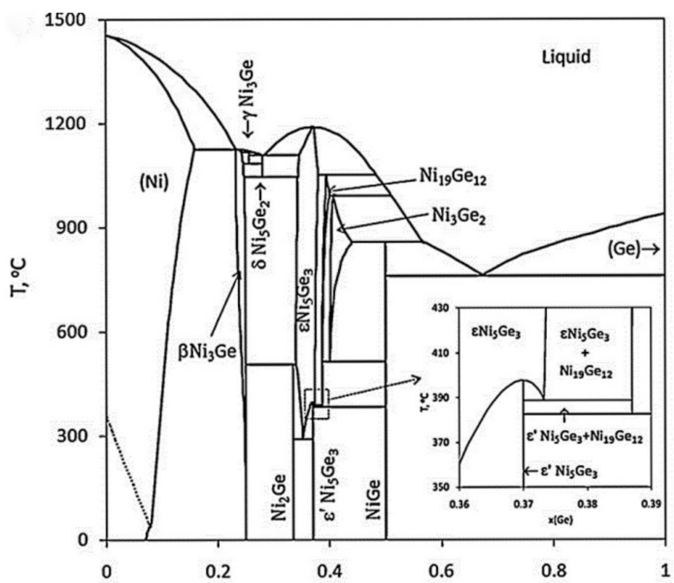

Fig.4. Calculated Ni-Ge phase diagram [12].

Due to the small spot size of FEG-SEM equipment, the accuracy in quantitative composition of the IMC layers from EDX analysis are probably degraded, especially when the IMC thickness is below 1 µm in Au-Ge solder joints. According to Ni-Ge phase diagram (Fig. 4), Ni_2Ge, Ni_5Ge_3 and NiGe phases may occur in this Au-Ge solder joints. Lang *et al.* reported that a duplex Ni_5Ge_3/NiGe layer was formed between Au-Ge solder and electroless Ni-P coating [6]. To prepare a TEM sample for precise composition results, FIB machining was used to fabricate a thin film (thickness < 100 μm) at the Ni-W-P/Au-Ge solder interface (marked in Fig. 3 a)) for following TEM observations. The microstructure of FIB sample is illustrated in Fig. 5.

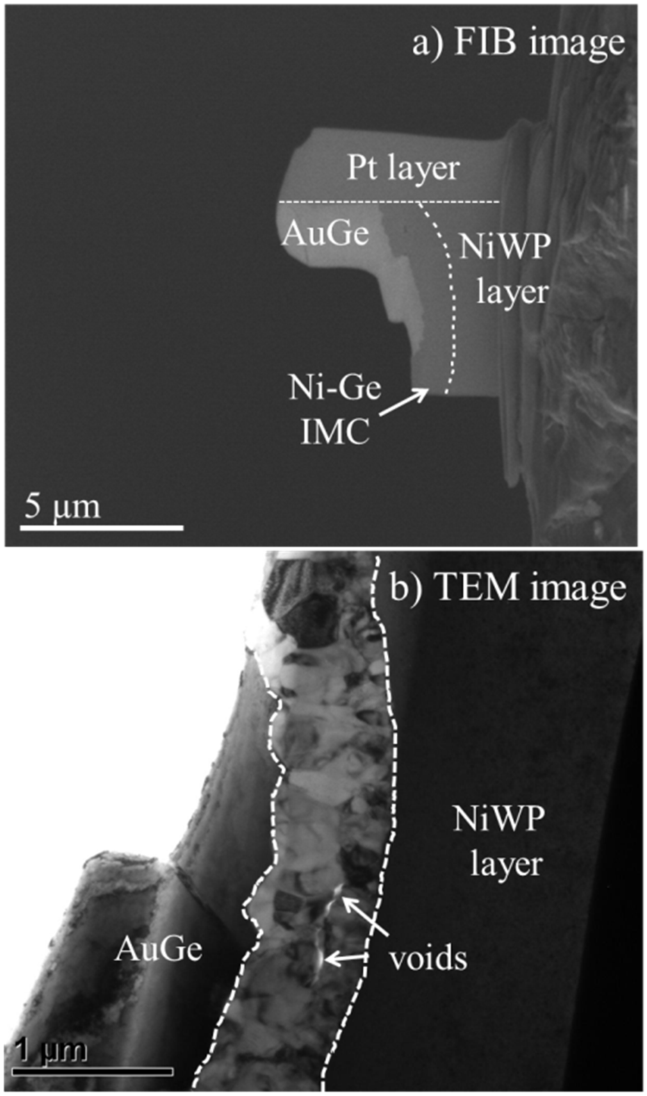

Fig. 5. FIB specimen at the Ni-W-P/Au-Ge interface from: a) FIB image; b) TEM bright-field image.

As shown in Fig. 5 a), this TEM sample consists of Au-12Ge solder, Ni-Ge IMCs and part of Ni-W-P layer. The top platinum (Pt) layer was for protection of the area of interests during FIB milling. The direction of the FIB milling was from top to bottom side with a beam current of 100 pA during the final thinning to minimise the effect of Ga implantation and contamination of milled materials on the sample surfaces [13]. The thickness of the TEM sample was approximately 96.9 nm, enabling precise and accurate results of TEM analysis including selected-area diffraction pattern (SADP), high resolution transmission electron microscopy (HRTEM) and EDX analysis at a nano-scale (over ×20000 magnification).

From the TEM bright-field image in Fig. 5 b), the IMC layer clearly generates at the Ni-W-P/Au-Ge interfaces in varying morphologies, including dendrite (~ 0.5 μm), scallop (~ 0.3 μm), and granular shape in the smallest size (50 nm approximately). According to the corresponding EDX results, although the shapes of IMC are different, they were all identified as Ni_5Ge_3 phase. No NiGe phase was found in this TEM sample, which is different from a previous work on the interfacial reactions between Au-Ge solder and electroless Ni-P coating [6]. However, NiGe IMC is still likely to generate in the Au-Ge solder joints because of the small area of selected TEM sample. Therefore, etching the Au-Ge solder away can be an effective method to discover the existence of NiGe grains. Besides, some small voids (<0.4 μm) were also formed near the IMC/Ni-W-P interface, as shown in Fig. 4 b), which is highly likely attributed to the poor wetting on this area.

C. Interfacial reaction and IMC morphology in aged Au-Ge solder joints

The interfacial reaction and morphological evolution in Au-Ge solder joints are shown in Fig. 6. For as-assembled samples, the IMC layer is consisted of two types of Ni-Ge IMCs; a darker layer close to solder part is NiGe with uneven heights, which exhibits a pyramid-like and polygon-like shape as shown in Fig. 6 b). The light layer close to Ni-W-P interlayer is identified as Ni_5Ge_3 in various shapes as discussed above through the TEM analysis. Moreover, the top-view micrographs and the corresponding EDS analysis prove the assumption that NiGe exists in as-built Au-Ge solder joints.

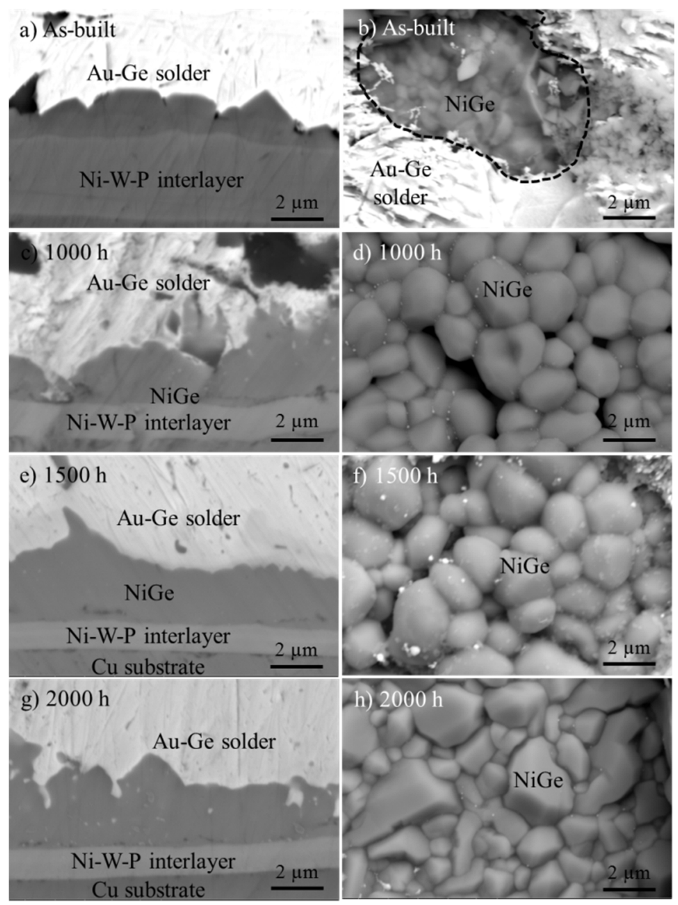

Fig. 6 Microstructural evolution for Ni-P solder joints: (a) cross section and (b) top view of as-assembled state; (c) cross section and (d) top view ageing for 1000h; (e) cross section and (f) top view ageing for 1500h; (g) cross section and (h) top view ageing for 2000h.

After ageing for 1000h at 300ºC, nearly half of this Ni-W-P coating was consumed by Au-Ge solder into formation of a thick layer of NiGe as shown in Fig. 6 c). As observed in Fig. 6 d), the NiGe grains exhibits granular morphology with an average diameter of 2 µm. By contrast, an electroless Ni-P coating with a 5µm thickness was completely consumed in Au-Ge solder joints under a same heating treatment as previously reported elsewhere [6]. Compared to Ni-P coating, this Ni-W-P layer shows better thermal stability and excellent diffusion barrier property. No visible voids and cracks were observed in this Ni-W-P coating as well.

While ageing for another 500h, the morphology of NiGe grains remained unaltered with a denser structure in Fig. 6 f). This agrees the microstructure from cross-sectional view in Fig. 6 e). Notably, the thickness of NiGe layer increase slightly from 2 µm to 2.35 µm, whereas the diameter of NiGe in top-view is still around 2 µm.

After the longest term of ageing (up to 2000h), it is interesting that the entire thickness of NiGe layer is stable at around 2.4 µm. However, the surface of this layer is rougher along with a coarser structure from a cross-section view.

In solid state reaction, the thickness of the IMC layer can be generally expressed:

$$\delta - \delta_0 = kt^{1/n} \quad (1)$$

Where δ and δ_0 is the thickness of NiGe layer at time t and zero, respectively. t is the solid-solid reaction duration, n is the time exponent, and k represents the growth rate constant of NiGe that can be calculated from the slope of the fit lines in Fig. 7.

Fig. 7 shows the relationship between the thickness of NiGe layer and the square root of ageing time at the Au-Ge/Ni-W-P. It is observed that the thickness of NiGe increases linearly with the square root of ageing time up to 1500h. This linear relationship (n =2) indicates that the growth mechanism of NiGe is diffusion-control during this ageing period. In this work, the growth rate coefficient of NiGe is calculated as 4.72×10^{-2} µm/h$^{1/2}$.

However, when annealing for 2000 h at 300ºC, the Ge elements from Au-Ge solder are almost fully reacted with Ni atoms in the Ni-W-P layer since the thickness of NiGe is rather stable at around 2.4 µm. This also leads to a polygon shape in a size range of 300 nm – 3 µm as shown in Fig. 6 h).

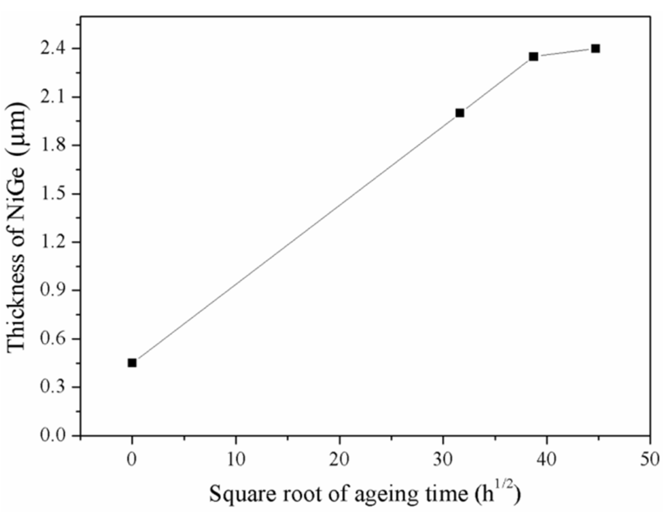

Fig. 7 Thickness of NiGe layer formed at Ni-W-P/Au-Ge solder interconnects during aging at 300ºC up to 2000h.

IV. Conclusions

In this work, an electroless ternary Ni-W-P alloy was developed and utilised as a diffusion barrier in high temperature solder joints. EDX compositional analysis illustrated that tungsten and phosphorus content in Ni-W-P coating were 15-16 wt.% and 6-7 wt.%, respectively. Interfacial reaction between Au-Ge solder and electroless Ni-W-P coating after reflow and prolonged ageing periods was investigated. Generally, Ni-W-P coating exhibits an excellent diffusion barrier property to prevent the mutual diffusions and reactions between Cu substrates and Au-Ge solders up to 2000 h. After reflow, two Au-Ge IMC layers (NiGe and Ni_5Ge_3) formed at the Ni-W-P/Au-Ge interface according to TEM analysis. However, after aging for 1000h, only NiGe grains were observed at the interface, while half of Ni-W-P coating was consumed by Au-Ge solder. The morphology of NiGe grains became in granular shape and remained unaltered subjected to 1500h ageing duration. After a fully consumption of Ge elements in solder part, the structure NiGe layer becomes coarser in cross-sectional view, while NiGe grains exhibit a polygon morphology with a diameter range of 300 nm – 3 µm from top view.

Acknowledgments

The authors would like to acknowledge the research grant funded through Centre of Power Electronics (CPE) of EPSRC via Nottingham University as well as FP7 Marie Curie IRSES Project, M6 (Grant No. PIRSES-GA-2010-269113). Thanks are also due to Mr. Scott Doak, Dr. Sabrina Yang in Loughborough Materials Characterisation Centre (LMCC) for their support on FIB training.

References

1. H.B. Qin, W.Y. Li, W.B. Zhou, and X.P. Zhang, “Low cycle fatigue performance of ball grid array structure Cu/Sn-3.0Ag-0.5Cu/Cu solder joints”, Microelectronics Reliability, vol. 54, No. 12, 2014, pp. 2911-2921.
2. Q.K. Zhang, H.F. Zou, and Z.F. Zhang, “Tensile and Fatigue Behaviors of Aged Cu/Sn-4Ag Solder Joints”, Journal of Electronic Materials, vol. 38, No. 6, 2009, pp. 852-859.
3. M. He, Z. Chen, and G. Qi, “Solid state interfacial reaction of Sn-37Pb and Sn-3.5Ag solders with Ni-P under bump metallization”, Acta Materialia, vol. 52, 2004, pp. 2047-2056.
4. K. Chen, C. Liu, D Whalley, and D. Hutt, “A comparative study of the interfacial reaction between electroless Ni-P coatings and molten tin”, Acta Materialia, vol. 56, 2008, pp. 5668-5676.
5. C.K. Chung, Y.J. Chen, T.L. Yang, and C.R. Kao, “Reactions of Sn-4.0Ag-0.5Cu on Cu and Electroless Ni Substrate in Premelting Soldering Process”, Journal of Electronic Materials, vol. 42, No. 6, 2013, pp. 1254-1259.
6. F.Q. Lang, H. Yamaguchi, H. Nakagawa, and H. Sato, “Solid-State Interfacial Reaction between Eutectic Au−Ge Solder and Cu Ni(P) Au Metalized Ceramic Substrate and Its Suppression”, Journal of Materials Science & Technology, vol. 31, 2015, pp. 445-452.
7. S.K. Tien, J.G. Duh, and Y.I. Chen, “The influence of thermal treatment on the microstructure and hardness in electroless Ni–P–W deposit”, Thin Solid Films, vol. 469-470, 2004, pp. 333–338.
8. D.M. Jang, and J. Yu, “Tungsten alloying of the Ni(P) films and the reliability of Sn–3.5Ag/NiWP solder joints”, Journal of Materials Research, vol. 26, No. 7, 2011, pp. 889-895.
9. J.N. Balaraju, Kalavati, N.T. Manikandanath, and V.K. William

Grips, “Phase transformation behavior of nanocrystalline Ni-W-P alloys containing various W and P contents”, Surface and Coatings Technology, vol. 206, No. 10, 2012, pp. 2682–2689.

10. Y. Yang, J.N. Balaraju, S.C. Chong, H. Xu, C. Liu, V.V. Silberschmidt, and Z. Chen, “Significantly retarded interfacial reaction between an electroless Ni–W–P metallization and lead-free Sn–3.5Ag solder”, Journal of Alloys and Compounds, vol. 565, 2013, pp. 11–16.
11. K. Chen, C. Liu, D.C. Whalley, and D.A. Hutt, “Electroless Ni-W-P alloys as barrier coating s for liquid solder interconnects”, in 1st Electronics System Integration Technology Conference (ESTC), Dresden, Germany, 2006, pp. 421-427.
12. Y.Q. Liu, D.J. Ma, Y. Du, “Thermodynamic modelling of the germanium-nickel system”, Journal of Alloys and Compounds, vol. 491, 2010, pp. 63-71.
13. D. Kiener, C. Motz, M. Rester, M. Jenko, and G. Dehm, “FIB damage of Cu and possible consequences for miniaturized mechanical tests”, Materials Science and Engineering A, vol. 459, 2007, pp. 262-272.